BASIC RESEARCH www.jasn.org

Fetuin-A Protects against Atherosclerotic Calcification in CKD

Ralf Westenfeld,* Cora Schäfer,† Thilo Krüger,* Christian Haarmann,* Leon J. Schurgers,‡ Chris Reutelingsperger,‡ Ognen Ivanovski,§ Tilman Drueke,§ Ziad A. Massy,‖ Markus Ketteler,¶ Jürgen Floege,* and Willi Jahnen-Dechent†

Departments of *Nephrology and †Biomedical Engineering, Rheinisch-Westfälische Technische Hochschule (RWTH) Aachen University Hospital, Aachen, and ¶Department of Nephrology, Klinikum Coburg GmbH, Coburg, Germany; ‡Department of Biochemistry, Cardiovascular Research Institute Maastricht, Maastricht, Netherlands; and §INSERM Unit 845, Necker Hospital, Paris, and ‖Inserm ERI-12 and University of Picardie Jules Verne and Amiens University Hospital, Amiens, France

ABSTRACT

Reduced serum levels of the calcification inhibitor fetuin-A associate with increased cardiovascular mortality in dialysis patients. Fetuin-A–deficient mice display calcification of various tissues but notably not of the vasculature. This absence of vascular calcification may result from the protection of an intact endothelium, which becomes severely compromised in the setting of atherosclerosis. To test this hypothesis, we generated fetuin-A/apolipoprotein E (ApoE)-deficient mice and compared them with ApoE-deficient and wild-type mice with regard to atheroma formation and extraosseous calcification. We assigned mice to three treatment groups for 9 wk: (*1*) Standard diet, (*2*) high-phosphate diet, or (*3*) unilateral nephrectomy (causing chronic kidney disease [CKD]) plus high-phosphate diet. Serum urea, phosphate, and parathyroid hormone levels were similar in all genotypes after the interventions. Fetuin-A deficiency did not affect the extent of aortic lipid deposition, neointima formation, and coronary sclerosis observed with ApoE deficiency, but the combination of fetuin-A deficiency, hyperphosphatemia, and CKD led to a 15-fold increase in vascular calcification in this model of atherosclerosis. Fetuin-A deficiency almost exclusively promoted intimal rather than medial calcification of atheromatous lesions. High-phosphate diet and CKD also led to an increase in valvular calcification and aorta-associated apoptosis, with wild-type mice having the least, ApoE-deficient mice intermediate, and fetuin-A/ApoE-deficient mice the most. In addition, the combination of fetuin-A deficiency, high-phosphate diet, and CKD in ApoE-deficient mice greatly enhanced myocardial calcification, whereas the absence of fetuin-A did not affect the incidence of renal calcification. In conclusion, fetuin-A inhibits pathologic calcification in both the soft tissue and vasculature, even in the setting of atherosclerosis.

J Am Soc Nephrol 20: 1264–1274, 2009. doi: 10.1681/ASN.2008060572

Hemodialysis (HD) patients experience a cardiovascular mortality of up to 20% per year, and vascular calcification is a strong independent risk factor of cardiovascular death.[1,2] Pathologic calcification is driven both by an elevated serum calcium phosphate product and by differentiation of vascular or mesenchymal cells into osteoblast-like cells, becoming mineralization competent.

Serum is a metastable solution with respect to calcium phosphate precipitation. Once started, calcification proceeds rapidly in the presence of calcifiable templates such as collagen, elastin, and cell debris.[3–5] Fetuin-A accounts for approximately 50% of the capacity of serum to inhibit the spontaneous apatite formation from solutions supersaturated in

Received June 5, 2008. Accepted January 19, 2009.

Published online ahead of print. Publication date available at www.jasn.org.

R.W. and C.S. contributed equally to this work.

Correspondence: Dr. Willi Jahnen-Dechent, Department of Biomedical Engineering, Biointerface Group, RWTH Aachen University Hospital, Pauwelsstrasse 30, 52074 Aachen, Germany. Phone: +49-241-80-80163; Fax: +49-241-80-82573; E-mail: willi.jahnen@rwth-aachen.de

calcium and phosphate.[6] The inhibition is achieved by rapid formation of soluble colloidal fetuin-A calcium phosphate complexes, termed calciprotein particles (CPPs).[7–9]

We previously showed that HD and calciphylaxis patients have depressed fetuin-A serum levels accompanied by a reduced capacity of their serum to inhibit calcium phosphate precipitation.[5] In cross-sectional studies in HD patients, fetuin-A deficiency was identified as an inflammation-related predictor of cardiovascular and all-cause mortality, respectively.[10,11] In patients without chronic kidney disease (CKD), fetuin-A levels correlated inversely with advanced coronary calcification.[12,13] Fetuin-A–deficient (Ahsg−/−) mice maintained on the DBA/2 background exhibit a fully penetrating phenotype with extensive soft tissue calcification, whereas C57BL/6 Ahsg−/− mice represent "borderline calcifying" mice whereby rapid calcification can be induced by additional metabolic challenges or induction of CKD.[5,14]

Calcification of the aorta or larger vessels is conspicuously absent in Ahsg−/− mice; therefore, the role for fetuin-A as an inhibitor of vascular calcification was uncertain.[15,16] Absent vascular calcification in Ahsg−/− mice may be related to the protective mechanisms by an intact endothelium, which is severely compromised in humans with atherosclerosis and thus may serve as a nidus for subsequent calcification. To test this hypothesis, we created Ahsg−/−/apolipoprotein E double-deficient (ApoE−/−) mice maintained on the C57BL/6 genetic background to dissect the contribution of fetuin-A, CKD, and an elevated calcium-phosphorus product (Ca × P) to the development of atheroma formation and vascular calcification in an established murine model of atherosclerosis.

RESULTS

Calcifying Atherosclerosis in Ahsg/−/−ApoE−/− Mice after Induction of CKD

In this study, we used a combination model of genetic fetuin-A deficiency and induced CKD caused by unilateral nephrectomy (Nx) plus high-phosphate (HP) diet in 8-mo-old mice. Interventions were performed in wild-type (wt), ApoE−/−, and Ahsg−/−/ApoE−/− mice, respectively, resulting in nine different groups. Mice generally recovered well from surgery. Mortality within the first 7 d after Nx was <10%. HP diet and especially HP-Nx treatment were associated with increased mortality at later time points and was most pronounced in ApoE−/− and Ahsg−/−/ApoE−/− mice, reaching 30% (Figure 1). Significant weight loss (Figure 1) was observed only after HP-Nx treatment and was comparable in all three genotypes (groups 3, 6, and 9 *versus* 1; $P < 0.001$). A total of 143 mice reached the end of the study.

Serum Chemistry

All mice that underwent unilateral Nx and were kept on an HP diet developed CKD. Disease was associated with roughly 25% increased blood urea nitrogen (BUN; groups 3, 6, and 9 *versus* 1; $P < 0.001$) and 40% increased creatinine (data not shown). Genotype or HP diet alone did not affect serum BUN or serum

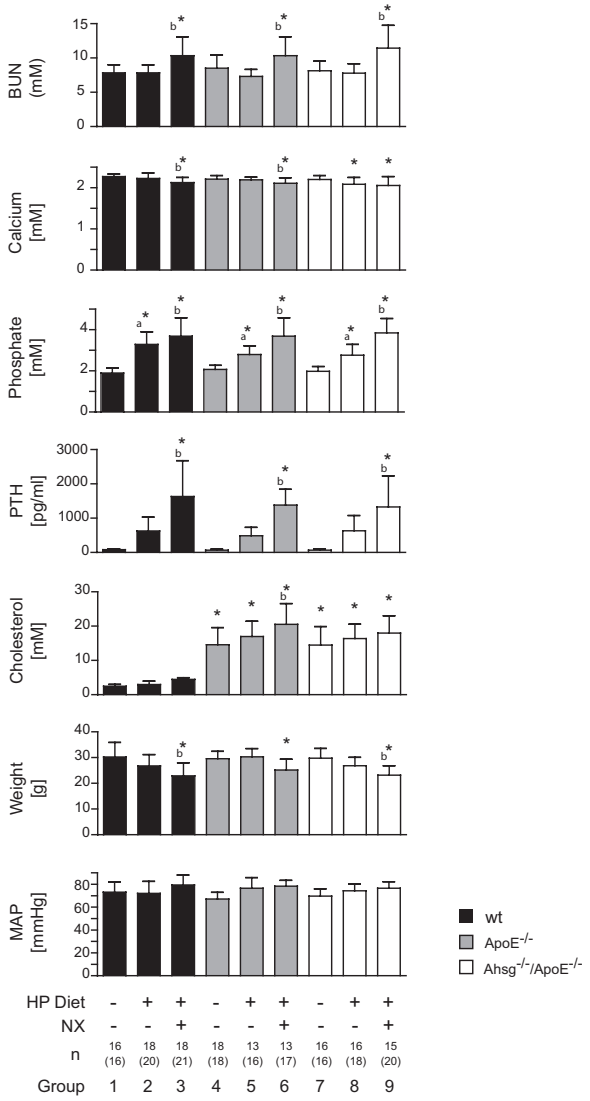

Figure 1. Serum chemistry, BUN, total calcium, phosphate, intact parathyroid hormone (PTH), total cholesterol, body weight, and mean arterial pressure (MAP) in various treatment groups of wt (■), ApoE−/− (▨), and Ahsg−/−/ApoE−/− (□) mice. The columns represent means ± SD. *$P < 0.05$ *versus* group 1; [a]$P < 0.05$ between low phosphorus (LP) and matched HP group (1 *versus* 2; 4 *versus* 5; 7 *versus* 8); [b]$P < 0.05$ between CKD and matched control group (1 *versus* 3; 4 *versus* 6; 7 *versus* 9). Numbers of mice reaching the end of the study as well as total animal numbers (in parentheses) of every group are given.

calcium levels (Figure 1, top two panels). HP diet did, however, increase serum phosphate. The rise was significant (30 to 50%) in nonoperated mice and attained frank hyperphosphatemia (100%) in the HP-Nx groups (groups 3, 6, and 9 *versus* 1; $P < 0.001$). Again, the genotype did not affect serum phosphate levels. HP diet was associated with a roughly five-fold increase of serum parathyroid hormone that was further increased (20-fold) upon HP-Nx treatment (groups 3, 6, and 9 *versus* 1; $P < 0.001$). Again, the changes were independent of genotypes. Serum calcium levels were reduced significantly in all mice after

HP-Nx treatment. This reduction was most pronounced in Ahsg−/−/ApoE−/− mice on HP-Nx (group 9 *versus* 1; $P < 0.001$). Likewise, serum albumin was reduced in Ahsg−/−/ApoE−/− mice upon HP-Nx treatment (group 9 *versus* 1; $P < 0.001$; data not shown). As expected, ApoE deficiency was associated with hypercholesterolemia. Fetuin-A deficiency did not affect cholesterol levels in Ahsg−/−/ApoE−/− mice (Figure 1). We detected a stepwise increase of serum cholesterol levels in all three genotypes upon HP treatment (15%) and upon HP-Nx treatment (40%), attaining statistical significance in ApoE−/− mice (group 6 *versus* 4; $P < 0.05$). Fetuin-A serum levels in wt mice were not affected by HP or HP-Nx treatment (data not shown).

Blood Pressure

Mean arterial pressure was similar in all genotypes of the same treatment groups (Figure 1, bottom). We detected a small rise in mean arterial pressure in HP-Nx–treated mice compared with control mice, which failed to reach statistical significance. We detected no statistically significant differences of systolic, diastolic, or pulse pressure measurements in the various treatment groups (data not shown).

Analysis of Atherosclerotic Lesions

We quantified atherosclerotic lesion development by histomorphometry of Oil Red O–stained *en face* preparations of thoracic aortas (Figure 2, A, D, E, and F). We also analyzed intimal lesion size on serial sections of the aortic root stained with Masson's trichrome (Figure 2, B, G, H, and I). Both techniques independently confirmed the observation that fetuin-A deficiency was not associated with atheroma formation in the aorta, whereas ApoE deficiency was always associated with atherosclerotic lesions. HP and HP-Nx treatment did not significantly change atheroma size (group 5 or 6 *versus* 4; group 8 or 9 *versus* 7). Atheroma plaque formation in ApoE−/− mice starts retrovalvular in the aortic sinus and gradually disperses toward the coronary arteries.[17,18] To quantify late plaque formation, we therefore investigated lesion progression in the common coronary arteries. We detected no difference in atheroma formation between ApoE−/− and Ahsg−/−/ApoE−/− mice (Figure 2, C, J, K, and L). Both genotypes showed coronary lesions in 50% of the mice, gradually increasing to 80% in HP-Nx mice (group 6 and 9). Only two of 18 wt mice exhibited coronary lesions after HP-Nx treatment, whereas all other wt mice had no coronary atheromas at all.

Vascular Calcification

We quantified vascular calcification using von Kossa–stained serial sections of the aortic root (Figure 3, A, D, E, and F). Wt mice exhibited small spotty calcifications that slightly increased in size and number in the HP-Nx treatment group. Ahsg−/−/ApoE−/− mice on HP diet sustained 10-fold increased aortic calcification compared with wt mice (group 8 *versus* 2; $P < 0.001$). Unilateral Nx in combination with HP diet was associated with a 15-fold increase in vascular calcification in Ahsg−/−/ApoE−/− mice compared with wt mice (group 9 *versus* 3; $P < 0.001$). Of note, the same treatment in ApoE−/− mice was associated with a significantly lower level of aortic calcification (group 9 *versus* 6; $P < 0.01$) than in Ahsg−/−/ApoE−/−;mice, demonstrating that fetuin-A deficiency enhanced vascular calcification in ApoE-deficient mice. Moreover, ulcerating calcifying plaques staining positive for AnnexinV indicative of apoptosis (Figure 3K) were more frequent in the aortas of double-deficient mice compared with wt and ApoE−/− mice (group 3: 5%; group 6: 30%; group 9: 65%; Figure 3, C and J). Quantitative histomorphometry of the common coronary arteries corroborated the enhanced vascular calcification phenotype of Ahsg−/−/ApoE−/− mice (Figure 3, B, G, H, and I): The greatest extent of coronary calcification was detected in the Ahsg−/−/ApoE−/− mice upon HP and HP-Nx treatment (Figure 3, B and I).

Phenotypic Characterization of Calcifying Aortic Tissue

A detailed analysis of calcification in the media layer of the aorta *versus* the intima/plaque area showed that the vast majority of calcification occurred in the intima/plaque area (Figure 4, A and B). The calcified part of the intima/plaque area of a typical cross-section of an aorta greatly increased with HP, Nx, and lack of fetuin-A. It attained values in excess of 100,000 μm^2, or 0.1 mm^2, when all three risk factors of calcification were combined (group 9). In contrast, the calcified part of a typical cross-section of an aorta was 100-fold lower and ranged from 800 to 3000 μm^2 in the media regardless of the treatment. The differences between treatment groups were statistically insignificant because of high variation and low incidence. Atherosclerotic calcification is associated with apoptosis of vascular or invaded cells that start and perpetuate pathogenesis. To assess the amount of apoptosis, we performed fluorescence terminal deoxynucleotidyl transferase–mediated digoxigenin-deoxyuridine nick-end labeling histochemistry on aorta sections. We expressed the amount of apoptosis as percentage of vascular wall area covered by positive signal, as detailed in Figure 3L. The autofluorescent elastic lamina was excluded from the analysis unless brightly fluorescent spots the size of cell nuclei were detected. Using histomorphometry, we determined that the area covered by apoptotic nuclei gradually increased from 0 in untreated mice to 1.5% in mice with the highest incidence of calcification (group 9; Figure 4C). Like the calcified lesions, apoptotic nuclei almost exclusively mapped to the intima/plaque area of the aorta sections. Usually, atherosclerotic calcification is associated with both macrophages and smooth muscle cells; therefore, we assessed calcification in the context of the cell type directly juxtaposed to it. We analyzed the differential gene expression of osteopontin (OPN; a marker for reactive macrophage activity[19]), matrix GLA protein (MGP; an aorta-specific inhibitor of media calcification[20]), and SM22-α (vascular smooth muscle cell marker) by quantitative reverse transcriptase–PCR. Figure 4, D through F, shows the fold change for each treatment group compared with untreated wt mice. OPN and MGP expression markedly in-

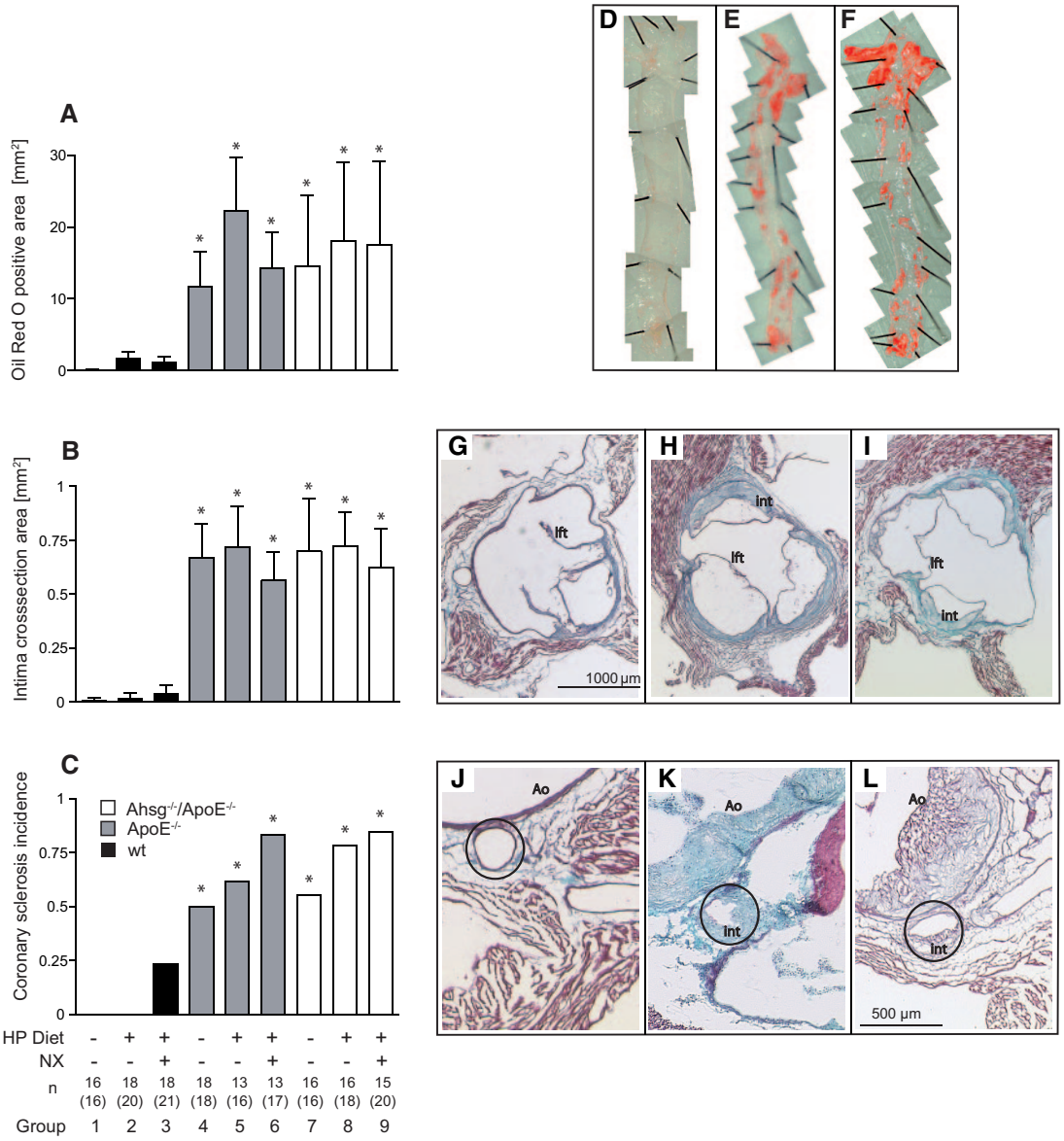

Figure 2. Atherosclerotic lesion histomorphometry at different vascular sites in wt (■), ApoE−/− (▨), and Ahsg−/−/ApoE−/− (□) mice and representative photomicrographs of *en face*–mounted Oil Red O–stained aortas or stained tissue sections. (A) Atherosclerotic lesion size estimated from Oil Red O–stained whole-mount aortas as depicted on the right for experimental groups 3, 6, and 9 (D, E, and F). (B) Intima thickness (int) determined from serial sections cut through the aortic root displaying the aortic sinus and the aortic valve leaflets (lft) after Masson's trichrome staining as depicted on the right for experimental groups 3, 6, and 9 (G, H, and I). (C) Incidence of coronary sclerosis. Representative sections of the experimental groups 3, 6, and 9 (J, K, and L) after Masson's trichrome staining depict proximal coronary arteries (circles). All values in groups 4 through 9 differed significantly from the matching values in groups 1 through 3 ($P < 0.05$). Numbers of mice reaching the end of the study as well as total animal numbers (in parentheses) of every group are given.

creased after HP-Nx treatment, especially in the Ahsg−/−/ApoE−/− mice. This finding confirmed and extended our previous study in fetuin-A single-deficient mice[14] in that OPN expression closely paralleled the steady increase in vascular calcification throughout the nine treatment groups (Figure 3D). MGP expression preceded calcification in that MGP was already upregulated by HP and HP-Nx in wt mice that barely showed calcification (groups 2 and 3). Interestingly, the highest increase of MGP expression occurred in HP-Nx–treated mice independent of genotype, suggesting that MGP upregulation may be a protective response in uremia-associated calcification, which is known to affect mostly the tunica media, the layer that naturally expresses the highest amount of MGP.[21] No change in SM22-α marker expression was visible, regardless of treatment.

Heart Calcification

We analyzed myocardial calcification using serial sections through the aortic root and von Kossa staining (Figure 5A, E, F,

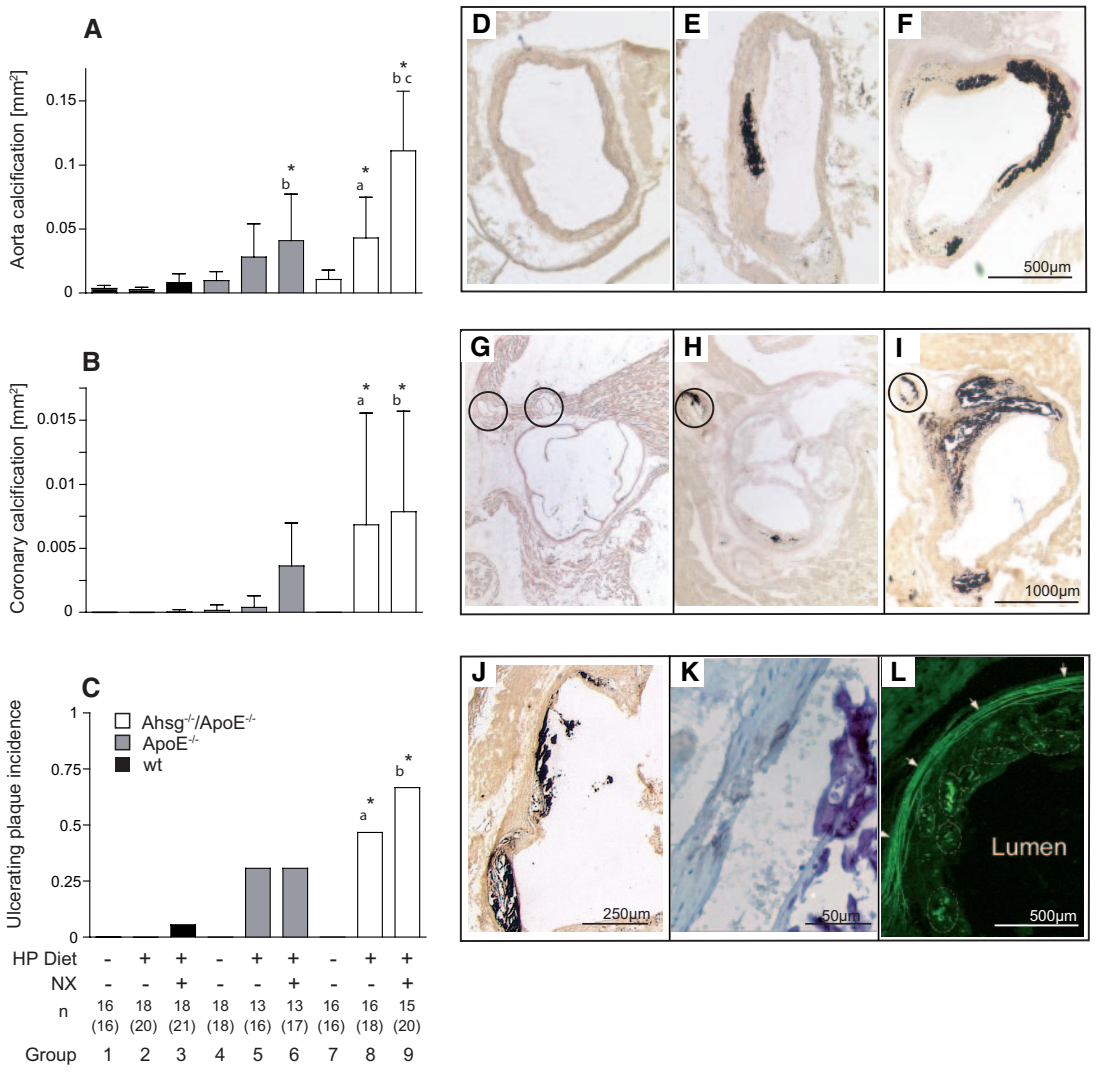

Figure 3. (A through C) Vascular calcification histomorphometry of von Kossa–stained tissue sections of (A) aorta calcification, (B) coronary artery calcification, and (C) ulcerating plaque incidence in the various treatment groups of wt (■), ApoE−/− (▨), and Ahsg−/−/ApoE−/− (□) mice. (D through I) Representative photomicrographs are depicted on the right for the treatment groups 3 (D and G), 6 (E and H), and 9 (F and I). (J) A type 5b calcified plaque stained with von Kossa. The tissue was not decalcified before sectioning and thus partially ruptured. (K) A similarly large calcified atherosclerotic lesion stained strongly positive with hematoxylin, suggesting proteinaceous calcified debris, and also AnnexinV (brown stain), indicating apoptosis close to the calcified border region of the plaque. (L) Apoptosis in the aorta wall was further analyzed by fluorescence terminal deoxynucleotidyl transferase–mediated digoxigenin-deoxyuridine nick-end labeling staining. Note that the elastic layer of the tunica media (white arrows) is autofluorescent. White broken lines encircle strongly positive nuclei of apoptotic cells in an extended atherosclerotic plaque (group 9). The columns in A through C represent means ± SD. *$P < 0.05$ *versus* group 1; $^{a}P < 0.05$ between LP and matched HP group (1 *versus* 2; 4 *versus* 5; 7 *versus* 8); $^{b}P < 0.05$ between CKD and matched control group (1 *versus* 3; 4 *versus* 6; 7 *versus* 9); $^{c}P < 0.05$ between Ahsg−/−/ApoE−/− and matched ApoE−/− group (4 *versus* 7; 5 *versus* 8; 6 *versus* 9). Numbers of mice reaching the end of the study as well as total animal numbers (in parentheses) of every group are given.

and G). Wt and ApoE−/− mice exhibited no visible calcification, not even on HP diet. Combined HP-Nx treatment induced small-size calcifications in approximately 10% of the wt mice and in 20% of the ApoE−/− mice, respectively. In contrast, myocardial calcification was shown in 25% of Ahsg−/−/ApoE−/− mice on HP diet, and combined HP-Nx treatment was associated with overt calcification in >90% of the Ahsg−/−/ApoE−/− mice (Figure 5, A and G).

The histologic results were confirmed by the chemical calcium analysis in myocardial tissue (Figure 5B). Wt and ApoE−/− mice showed no significant increase in tissue calcium after HP or HP-Nx treatment. In contrast, Ahsg−/−/ApoE−/− mice displayed severe tissue calcification on HP-Nx treatment with a 20-fold increase in tissue calcium (group 9 *versus* all other groups; $P < 0.001$).

Next, we quantified aortic valve calcification by histomor-

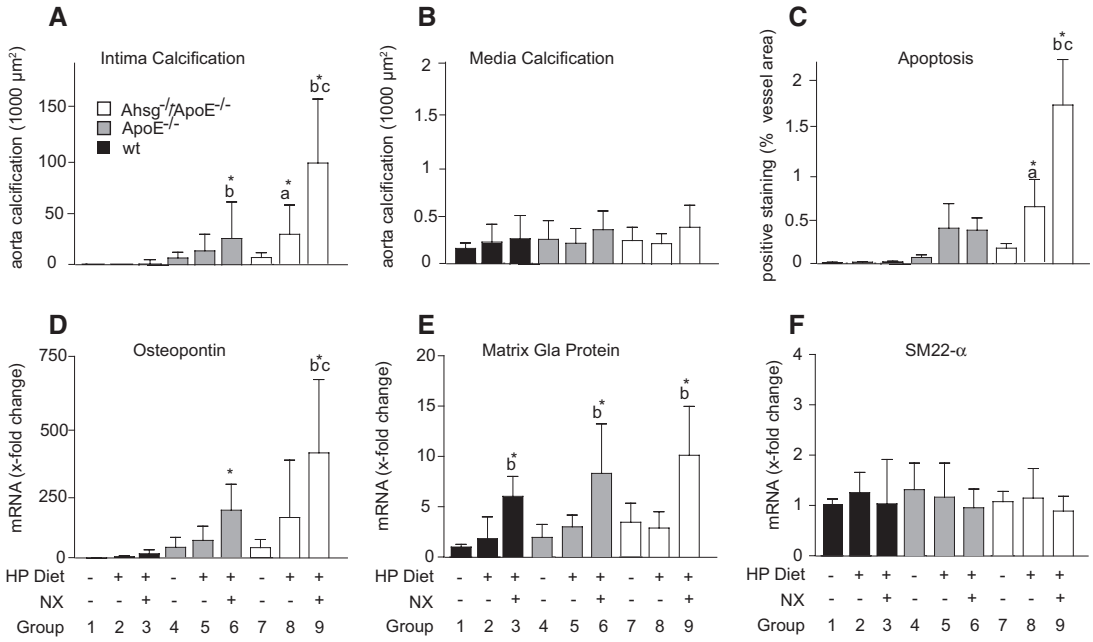

Figure 4. (A and B) Phenotypic characterization of calcifying aorta tissue. (C) Apoptosis was assessed histochemically and expressed as percentage of vascular wall area. (D through F) Differential expression of OPN (marker for reactive macrophage activity; D), MGP (tissue restricted inhibitor of media calcification; E), and SM22-α (vascular smooth muscle cell marker; F). mRNA was analyzed by quantitative reverse transcriptase–PCR as detailed in the Concise Methods section. Shown is the fold change compared with untreated wt mice. The columns represent means ± SD. $^{*}P < 0.05$ *versus* group 1; $^{a}P < 0.05$ between LP and matched HP group (1 *versus* 2; 4 *versus* 5; 7 *versus* 8); $^{b}P < 0.05$ between CKD and matched control group (1 *versus* 3; 4 *versus* 6; 7 *versus* 9); $^{c}P < 0.05$ between Ahsg−/−/ApoE−/− and matched ApoE−/− group (4 *versus* 7; 5 *versus* 8; 6 *versus* 9). Histologic sections and mRNA expression levels were scored in 10 mice for each treatment group.

phometry using serial sections through the aortic root and von Kossa staining. We detected a gradual increase of calcified valve area, which was positively correlated with the HP and Nx treatments as well as with ApoE and Ahsg genotypes (Figure 5C). Compared with wt mice, a significant increase in aortic valve calcification was identified in ApoE−/− and Ahsg−/−/ApoE−/− mice upon HP as well as HP-Nx treatment. Again, Ahsg−/−/ApoE−/− mice upon HP-Nx treatment exhibited the highest increase in valvular calcification, reaching a five-fold increase compared with wt control mice (group 9 *versus* 1; $P < 0.001$).

Kidney Calcification

Renal tissue calcium content was indistinguishable in all control mice (groups 1, 4, and 7) ranging from 2.1 to 3.4 mg/g dry wt. Likewise, renal calcium content in all three genotypes studied increased on HP diet (12-fold, group 1 *versus* 2, 5, and 8) and combined HP-Nx treatment (40-fold, group 1 *versus* 3, 6, and 9; $P < 0.001$; Figure 5).

DISCUSSION

In this study, we assessed the role of fetuin-A in the development of vascular calcification using various combinations of fetuin-A deficiency, high dietary phosphate administration, mild renal failure, and murine atherosclerosis. Importantly, these studies were performed on the relatively calcification-resistant genetic background C57BL/6,[22] allowing us to test interventions further aggravating calcification, which would not have been possible in mice with the calcification-prone DBA/2 background. In our study, we first ascertained that fetuin-A deficiency did not alter atherosclerosis formation when combined with ApoE−/− mice, a well-established murine model of atherosclerosis. In addition, we also found that fetuin-A deficiency added to the ApoE−/− genotype did not affect the calcium-phosphate metabolism and the development of secondary hyperparathyroidism, at least during the course of the study. The model therefore seems suitable to investigate the relative contributions of fetuin-A, atherosclerotic vascular damage, hyperphosphatemia, and CKD to extraosseous calcification.

The major finding of this study is that the combination of atherosclerotic vascular damage, hyperphosphatemia, and CKD with fetuin-A deficiency leads to a marked increase in vascular calcification. The data extend our previous work, which showed that the combination of hyperphosphatemia, CKD, and fetuin-A deficiency in C57BL/6 mice augmented extraosseous calcifications, for example, in the myocardium but spared the vasculature.[14] Thus, this model is more in line with the human situation, whereby depressed fetuin-A levels are particularly devastating in patients who have CKD with

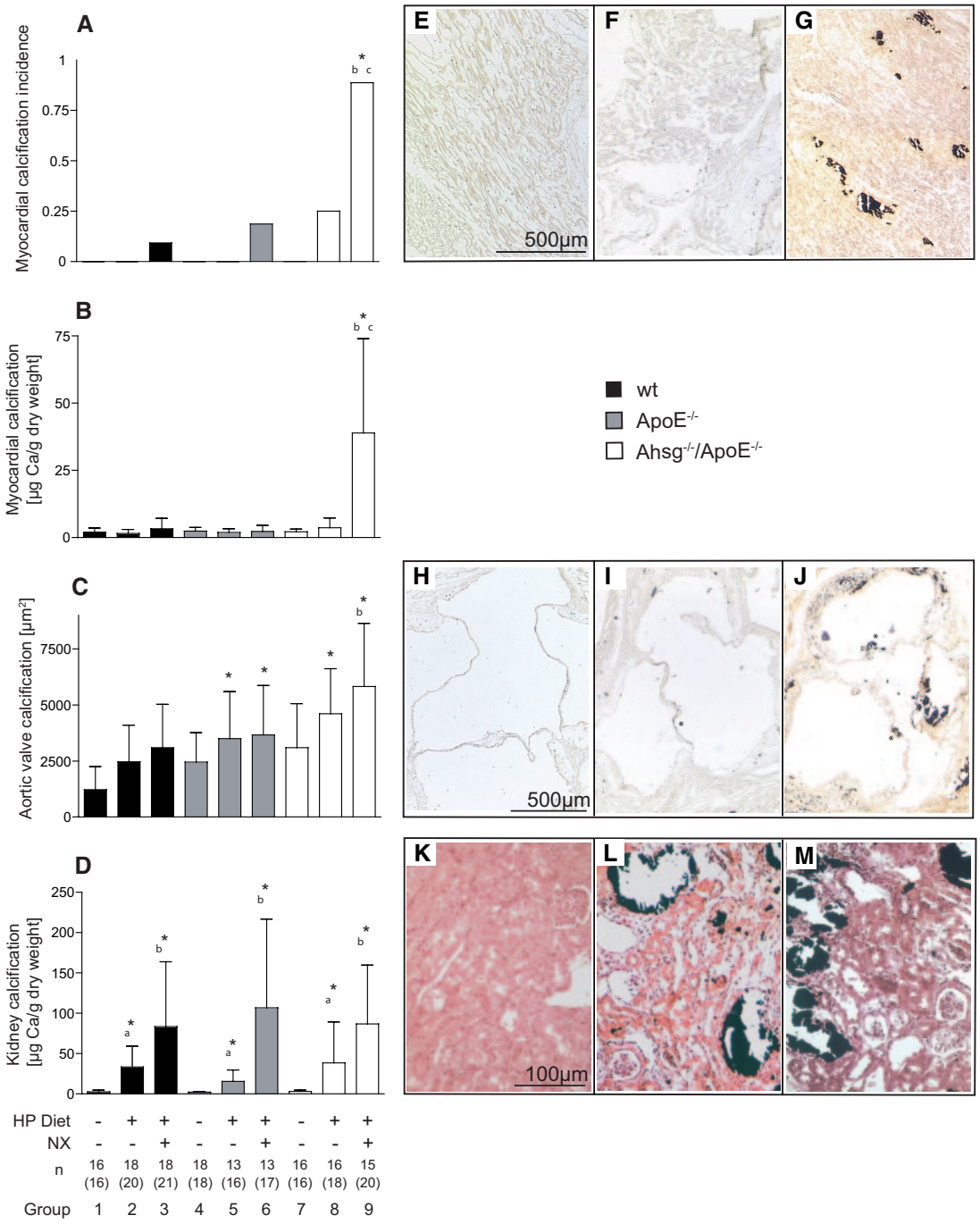

Figure 5. Soft tissue calcification quantified by calcium analysis of tissue extracts and illustrated by von Kossa–stained tissue sections in various treatment groups of wt (■), ApoE−/− (▨), and Ahsg−/−/ApoE−/− (□) mice. (A and B) Myocardial calcification incidence and extent, respectively. (C) Aortic valve calcification. (D) Kidney calcification. (E through M) Representative photomicrographs are depicted on the right for the treatment groups 3 (E, H, and K), 6 (F, I, and L) and 9 (G, J, and M). The columns represent means ± SD. *$P < 0.05$ *versus* group 1; [a]$P < 0.05$ between LP and matched HP group (1 *versus* 2; 4 *versus* 5; 7 *versus* 8); [b]$P < 0.05$ between CKD and matched control group (1 *versus* 3; 4 *versus* 6; 7 *versus* 9); [c]$P < 0.05$ between Ahsg−/−/ApoE−/− and matched ApoE−/− group (4 *versus* 7; 5 *versus* 8; 6 *versus* 9). Numbers of mice reaching the end of the study as well as total animal numbers (in parentheses) of every group are given.

associated increases in calcium and phosphorus load. In this population, depressed fetuin-A serum levels are associated with more extensive vascular[23] and valvular[24] calcification in cross-sectional analyses and with increased cardiovascular and all-cause mortality longitudinally.[10,11,25] This experimental work is also in accordance with recent epidemiologic studies in

humans demonstrating that reduced fetuin-A serum levels are associated with higher incidence of valvular calcification in patients with coronary artery disease, even in the absence of CKD.[13]

Our second major finding is that fetuin-A deficiency almost exclusively enhanced intimal calcification of atheromatous lesions. Calcification strongly correlated with the extent of apoptosis in the calcifying intima lesions and with the amount of OPN expressed. Assuming that the continued buildup of calcified debris in the absence of fetuin-A may cause apoptosis in macrophages as it does in smooth muscle cells,[26] it is tempting to speculate that calcification greatly enhances the vicious cycle of phagocytosis, apoptosis, *etc.* so well established in atherosclerosis-promoting macrophages laden with oxidized lipids.[27] Intimal calcification patterns characterize older patients with CKD,[28] whereas younger patients typically exhibit calcifications of the vascular media.[29] Our murine observations suggest that fetuin-A may help to prevent intima calcification but has little influence on media calcification and, as an alternative explanation, that only the intima, not the media, is damaged in this murine model and that such damage is a prerequisite for calcification. Furthermore, our observations point to maintained protection of the vascular media even in the combination of double-deficient mice with hyperphosphatemia and CKD. A prime candidate in this respect is the local calcification inhibitor MGP, which mainly influences media calcification.[21,30] Interestingly, MGP was most strongly upregulated after HP/Nx treatment, even in wt mice (Figure 4E, groups 3, 6, and 9) suggesting that MGP upregulation may be an adaptive response preventing imminent media calcification. Against this background, studies on the regulation and activation state of MGP in calcifying Ahsg−/−/ApoE−/− mice will be of interest to gain further insight into a potential collaboration of calcification inhibitory proteins.

The third major finding was that the combination of fetuin-A deficiency, HP diet, and CKD in ApoE−/− mice greatly enhanced myocardial calcifications, whereas renal calcifications were independent of the fetuin-A genotype. Myocardial calcifications were exacerbated to an extent, which already had been shown to induce myocardial stiffness, cardiac fibrosis, diastolic dysfunction, and catecholamine resistance in fetuin-A–deficient mice on the calcification-prone genetic background DBA/2.[16] The role of ApoE deficiency seems low in this context, because we showed previously that one of the key consequences of combining hyperphosphatemia and CKD in fetuin-A–deficient C57BL/6 mice was enhanced calcification of the myocardium.[14]

Taken together, a clear picture of fetuin-A in the prevention of soft tissue and vascular calcification emerges, in that fetuin-A exerts a decisive role as an inhibitor of pathologic calcification at multiple stages of disease progression: First, fetuin-A together with further acidic serum proteins acts as a mineral chaperone stabilizing colloidal calcium phosphate complexes as CPPs.[7,9] Calcium phosphate stabilization in the form of CPPs is cytoprotective in that it prevents vascular smooth muscle cell and presumably also macrophage apoptosis triggered by calcium phosphate.[26] This slows down atheroma formation, which—like calcification—is much faster in a dystrophic environment rich in apoptotic and necrotic cells.[31] In the absence of fetuin-A as a stabilizer of CPP and enhancer of apoptotic cell clearing,[32] remodeling is inefficient and calcified cellular debris accumulates into calcified lesions. Progressively, the environment of calcified atherosclerotic lesions may trigger osteogenic differentiation of tissue resident[26,33] or circulating mesenchymal precursor cells,[34,35] thereby turning calcification into true osteogenesis as in human cardiac valves.[36] We did not observe true bone formation in any of the calcified lesions of our mice despite strong expression of the bone-related protein OPN in fetuin-A–deficient mice.[14,19] We suggest that OPN is mainly produced by reactive macrophages in an attempt to clear the calcified lipidic debris.[3,19] Others have reported true osteogenesis and calcifying chondrogenesis in ApoE-deficient mice[37] and LDL receptor–deficient mice, respectively.[38] Unlike here, those mice however, were, fed a proatherogenic diet. Vascular osteogenesis as observed in humans is a late event in disease progression and may simply take more time to develop than the lifespan of mice on normal diet.

We conclude that the Ahsg−/−/ApoE−/− mice may be ideally suited to elucidate the contribution of various risk factors of cardiovascular disease, including the role of circulating mesenchymal precursors in the pathology of vascular calcification. Furthermore, this *in vivo* model of vascular and dystrophic tissue calcification may serve as a valuable test ground for therapeutic strategies.

CONCISE METHODS

Animals and Diets

The local animal welfare committee approved our animal study protocol. We generated Ahsg−/−/ApoE−/− mice by mating Ahsg−/− mice (B6-Ahsg^{tm1wja} N15) with ApoE−/− mice (B6.129P2-ApoE^{tm1Unc} N11), purchased from Taconic (Tornbjerg, Denmark)). Both strains were maintained on a C57BL/6 genetic background. Genotyping was performed by PCR of fetuin-A[5] or ApoE[39] as published. Mice were maintained in a temperature-controlled room on a 12-h day/night cycle. Food and water were given *ad libitum*. Before entering the study, all mice received standard phosphate chow (Altromin 1324; Altromin GmbH, Lage, Germany) containing 0.9% calcium, 0.7% Pi, 4% fat, and 19% protein (mainly soy grist). Mice receiving HP diet (Altromin C1049) containing 0.95% calcium, 1.65% phosphate, 4.5% fat, and 17% protein (mainly casein) were switched from standard phosphate to HP diet 1 wk after unilateral Nx or no operation. Mice were killed 9 wk after surgery; 143 mice reached the end of the study. Altogether, nine treatment groups entered the analysis. Wt mice on standard diet comprised group 1, on HP diet group 2, and on HP-Nx treatment group 3. ApoE−/− mice treated accordingly comprised groups 4 through 6, and Ahsg−/−/ApoE−/− mice treated accordingly comprised groups 7 through 9, as detailed in the figures.

Surgical Procedures

Mild CKD was achieved by unilateral Nx. Mice 8 mo of age were anesthetized by intraperitoneal injection with ketamine/xylazine (100 mg of ketamine and 5 mg of xylazine per kg body weight) and subjected to left-sided Nx. The mice generally recovered well from surgery; perioperative mortality was <10%. Mice were fed standard chow or HP diet for 9 wk. At the end of the experiments, mice were anesthetized with isoflurane, exsanguinated, and perfused with 10 ml of PBS; and kidney, heart, and aortic tissues were collected. For histologic analysis and detection of aortic calcification, the heart with the aortic root was separated from the distal aorta and snap-frozen as described previously.[40] One half of each kidney was separately fixed in 10% buffered formalin. The remaining tissues (heart and kidney) were processed for chemical analysis.

Systemic Parameters

Systemic BP was determined using an automated tail-cuff system (BP-2000 Series II Blood Pressure Analysis System; http://www.visitechsystems.com) in conscious mice that were acclimated to the procedure according to the standard protocol of the Jackson Laboratory (http://pga.jax.org/protocol_005.html). Each measurement was repeated three times for every mouse. The mice were weighed at the beginning and at the end of the experiment. Blood was drawn by retro-orbital bleeding. Serum was harvested by centrifugation at $1000 \times g$ and stored at −80°C until assayed for Ca, Pi, C-reactive protein, albumin, cholesterol, and BUN as described previously.[5] Parathyroid hormone was determined by a commercial ELISA (Immutopics, San Clemente, CA). Fetuin-A serum levels were determined by immunoblotting. Serum was fractionated on 10% polyacrylamide gels, blotted to nitrocellulose, and probed with polyclonal rabbit anti-mouse fetuin-A antibody at a dilution of 1:5000 in ABC buffer (PBS with 5% skim milk and 0.1% Tween 20) for 1 h at 37°C. After washing the blots with PBS including 0.1% Tween 20, secondary antibody conjugated with horseradish peroxidase (Vector Laboratories, Burlingame, Ca) was added at a dilution of 1:5000 in ABC buffer for 1 h at 37°C. Bound antibody was detected by chemiluminescence using luminol and x-ray film. Fluorographs were analyzed using a flatbed scanner and the Multianalysis software package (Biorad, Munich, Germany).

Quantification of Atherosclerotic Lesions

Cryosections, 8 μm thick, were cut from the proximal aorta starting at the end of the aortic sinus. Cryosections were stained with Oil Red O and counterstained with hematoxylin (Sigma, Taufkirchen, Germany). Adjacent sections were stained with Masson's trichrome stain for fibrosis and with von Kossa stain for calcification as described previously.[14] Quantitative analysis of lesions was performed using ImageJ histomorphometry software on at least six sections from each mouse. Morphology of the coronary artery was investigated on the descending part of the proximal vessels where the vessel diameter was >250 μm. The degree of atherosclerosis of the entire aorta was determined using Oil Red O staining of *en face*–prepared aortas as described previously with minor modifications.[40] Briefly, the mice were perfused with ice-cold PBS, and the thoracic aorta was removed, pinned out flat on a wax surface, sliced open starting from the aortic root, and stained with Oil Red O. The aortas were then photographed, and the entire lesion areas were measured by histomorphometry using ImageJ software.

Quantification of Apoptosis

Cryosections cut through the aortic root at the level of the aortic valve were chosen for analysis and stained with the *in situ* cell death detection kit according to the instructions (Roche Applied Sciences, Mannheim, Germany). Quantification of positive fluorescence was performed with computer-aided fluorescence microscopy (ImageJ software) and normalized to the total area of the vessel wall. Autofluorescence of the elastic lamellae in the tunica media was neglected.

RNA Isolation and Quantitative Reverse Transcription Real-Time PCR

Messenger RNA was extracted using commercial kits RNAlater and RNeasy (Qiagen, Hilden, Germany) with proteinase K digestion before RNA extraction to maximize mRNA yield. Integrity and amount of mRNA were analyzed by capillary electrophoresis (Agilent Bioanalyzer 2100; Agilent Technologies, Böblingen, Germany). Reverse transcription and real-time PCR were performed with the ABI 7700 sequence detection system (PE, Applied Biosystems, Foster City, CA) as described previously in detail.[16] Intron-spanning primers were derived from EnsEmbl for OPN (ENSMUST00000031243; sense GACCATGAGATTGGCAGTGATTT, antisense GATCTGGGTGCAGGCTGTAAAG, probe FAM-ATTGCCTCCTCCCTCCCGGTG-TAMRA) to yield an amplicon length of 116 bp; for MGP (ENSMUST00000032342; sense GCAGAGGTGGCGAGCTAAAG, antisense AGCGCTCACACAGCTTGTAGTC, probe FAM-AGAGTCCAGGAACGCAACAAGCCTGC-TAMRA) to yield an amplicon length of 104 bp, and for SM22-α (ENSMUST00000034590; sense ACGATGGAAACTACCGTGGAGAT, antisense GGCCTTCCCTTTCTAACTGATGA, probe FAM-TGAAGTCCCTCTTATGCTCCTGGGCTTTCT-TAMRA) to yield an amplicon length of 197 bp. Glyceraldehyde-3-phosphate dehydrogenase (GAPDH) primers were derived from EnsEmbl entry ENSMUST00000086934 (sense GGCAAATTCAACGGCACAGT, antisense AGATGGTGATGGGCTTCCC, probe FAM-AAGGCCGAGAATGGGAAGCTTGTCATC-TAMRA) to yield an amplicon length of 74 bp. Absolute mRNA quantification of samples was achieved by co-amplification of known quantities of pGEM-T plasmids (Promega, Madison, WI) containing the cloned target genes (GAPDH, OPN, MGP, and SM22-α). Expression was normalized to 1 million copies of GAPDH mRNA determined from the identical mRNA sample in each case. The expression level in untreated wt mice was arbitrarily assigned the value 1.0, and all other expression values were expressed as fold changes thereof.

Quantification of Soft Tissue Calcification

Calcium was extracted overnight using 0.6 M HCl. After clearing the tissue extracts by centrifugation ($10{,}000 \times g$ for 3 min), calcium was determined using cresolphthalein complexone chemistry and a commercial kit (Randox Laboratories Ltd., Crumlin, England).

Statistical Analysis

ANOVA with Tukey *post hoc* analysis was performed using GraphPad Prism software (GraphPad, San Diego, CA) to estimate overall differences in non–size-matched experimental groups. Confidence intervals >95% were regarded as significant.

ACKNOWLEDGMENTS

This work was funded by grants from Deutsche Forschungsgemeinschaft (Ja562/10) and the Interdisciplinary Center for Clinical Research (IZKF BioMAT; TV B67) of the Faculty of Medicine at the Rheinisch Westfälische Technische Hochschule (RWTH) Aachen University (R.W., V.B., and M.K.). Work at the Department of Biomedical Engineering in Maastricht was supported by grant 902-16-276 from the Medical Section of the Netherlands Organization for Scientific Research.

We thank Katrin Härthe and Nicole Bataille for excellent technical assistance.

DISCLOSURES

None.

REFERENCES

1. Collins AJ, Li SL, Ma JZ, Herzog C: Cardiovascular disease in end-stage renal disease patients. *Am J Kidney Dis* 38: S26–S29, 2001
2. Blacher J, Guerin AP, Pannier B, Marchais SJ, London GM: Arterial calcifications, arterial stiffness, and cardiovascular risk in end-stage renal disease. *Hypertension* 38: 938–942, 2001
3. Ghadially FN: As you like it: Part 3—A critique and historical review of calcification as seen with the electron microscope. *Ultrastruct Pathol* 25: 243–267, 2001
4. Murshed M, Harmey D, Millan JL, McKee MD, Karsenty G: Unique coexpression in osteoblasts of broadly expressed genes accounts for the spatial restriction of ECM mineralization to bone. *Genes Dev* 19: 1093–1104, 2005
5. Schäfer C, Heiss A, Schwarz A, Westenfeld R, Ketteler M, Floege J, Müller-Esterl W, Schinke T, Jahnen-Dechent W: The serum protein alpha 2-Heremans-Schmid glycoprotein/fetuin-A is a systemically acting inhibitor of ectopic calcification. *J Clin Invest* 112: 357–366, 2003
6. Schinke T, Amendt C, Trindl A, Pöschke O, Müller-Esterl W, Jahnen-Dechent W: The serum protein alpha2-HS glycoprotein/fetuin inhibits apatite formation *in vitro* and in mineralizing calvaria cells: A possible role in mineralization and calcium homeostasis. *J Biol Chem* 271: 20789–20796, 1996
7. Heiss A, DuChesne A, Denecke B, Grötzinger J, Yamamoto K, Renné T, Jahnen-Dechent W: Structural basis of calcification inhibition by alpha 2-HS glycoprotein/fetuin-A: Formation of colloidal calciprotein particles. *J Biol Chem* 278: 13333–13341, 2003
8. Heiss A, Jahnen-Dechent W, Endo H, Schwahn D: Structural dynamics of a colloidal protein-mineral complex bestowing on calcium phosphate a high solubility in biological fluids. *Biointerphases* 2: 16–20, 2007
9. Heiss A, Eckert T, Aretz A, Richtering W, van Dorp W, Schäfer C, Jahnen-Dechent W: Hierarchical role of fetuin-a and acidic serum proteins in the formation and stabilization of calcium phosphate particles. *J Biol Chem* 283: 14815–14825, 2008
10. Ketteler M, Bongartz P, Westenfeld R, Wildberger JE, Mahnken AH, Bohm R, Metzger T, Wanner C, Jahnen-Dechent W, Floege J: Association of low fetuin-A (AHSG) concentrations in serum with cardiovascular mortality in patients on dialysis: A cross-sectional study. *Lancet* 361: 827–833, 2003
11. Hermans MM, Brandenburg V, Ketteler M, Kooman JP, van der Sande FM, Boeschoten EW, Leunissen KM, Krediet RT, Dekker FW: Association of serum fetuin-A levels with mortality in dialysis patients. *Kidney Int* 72: 202–207, 2007
12. Lehtinen AB, Burdon KP, Lewis JP, Langefeld CD, Ziegler JT, Rich SS, Register TC, Carr JJ, Freedman BI, Bowden DW: Association of alpha2-Heremans-Schmid glycoprotein polymorphisms with subclinical atherosclerosis. *J Clin Endocrinol Metab* 92: 345–352, 2007
13. Ix JH, Chertow GM, Shlipak MG, Brandenburg VM, Ketteler M, Whooley MA: Association of fetuin-A with mitral annular calcification and aortic stenosis among persons with coronary heart disease: Data from the Heart and Soul Study. *Circulation* 115: 2533–2539, 2007
14. Westenfeld R, Schäfer C, Smeets R, Brandenburg VM, Floege J, Ketteler M, Jahnen-Dechent W: Fetuin-A (AHSG) prevents extraosseous calcification induced by uraemia and phosphate challenge in mice. *Nephrol Dial Transplant* 22: 1537–1546, 2007
15. Burke AP, Kolodgie FD, Virmani R: Fetuin-A, valve calcification, and diabetes: What do we understand? *Circulation* 115: 2464–2467, 2007
16. Merx MW, Schäfer C, Westenfeld R, Brandenburg V, Hidajat S, Weber C, Ketteler M, Jahnen-Dechent W: Myocardial stiffness, cardiac remodeling, and diastolic dysfunction in calcification-prone fetuin-A-deficient mice. *J Am Soc Nephrol* 16: 3357–3364, 2005
17. Nakashima Y, Plump AS, Raines EW, Breslow JL, Ross R: ApoE-deficient mice develop lesions of all phases of atherosclerosis throughout the arterial tree. *Arterioscler Thromb* 14: 133–140, 1994
18. Hu W, Polinsky P, Sadoun E, Rosenfeld ME, Schwartz SM: Atherosclerotic lesions in the common coronary arteries of ApoE knockout mice. *Cardiovasc Pathol* 14: 120–125, 2005
19. Jahnen-Dechent W, Schäfer C, Ketteler M, McKee MD: Mineral chaperones: A role for fetuin-A and osteopontin in the inhibition and regression of pathologic calcification. *J Mol Med* 86: 379–389, 2008
20. Luo G, Ducy P, McKee MD, Pinero GJ, Loyer E, Behringer RR, Karsenty G: Spontaneous calcification of arteries and cartilage in mice lacking matrix GLA protein. *Nature* 386: 78–81, 1997
21. Murshed M, Schinke T, McKee MD, Karsenty G: Extracellular matrix mineralization is regulated locally: Different roles of two gla-containing proteins. *J Cell Biol* 165: 625–630, 2004
22. Qiao JH, Xie PZ, Fishbein MC, Kreuzer J, Drake TA, Demer LL, Lusis AJ: Pathology of atheromatous lesions in inbred and genetically engineered mice: Genetic determination of arterial calcification. *Arterioscler Thromb* 14: 1480–1497, 1994
23. Moe SM, Reslerova M, Ketteler M, O'Neill K, Duan D, Koczman J, Westenfeld R, Jahnen-Dechent W, Chen NX: Role of calcification inhibitors in the pathogenesis of vascular calcification in chronic kidney disease (CKD). *Kidney Int* 67: 2295–2304, 2005
24. Wang AY, Woo J, Lam CW, Wang M, Chan IH, Gao P, Lui SF, Li PK, Sanderson JE: Associations of serum fetuin-A with malnutrition, inflammation, atherosclerosis and valvular calcification syndrome and outcome in peritoneal dialysis patients. *Nephrol Dial Transplant* 20: 1676–1685, 2005
25. Stenvinkel P, Wang K, Qureshi AR, Axelsson J, Pecoits-Filho R, Gao P, Barany P, Lindholm B, Jogestrand T, Heimburger O, Holmes C, Schalling M, Nordfors L: Low fetuin-A levels are associated with cardiovascular death: Impact of variations in the gene encoding fetuin. *Kidney Int* 67: 2383–2392, 2005
26. Reynolds JL, Joannides AJ, Skepper JN, McNair R, Schurgers LJ, Proudfoot D, Jahnen-Dechent W, Weissberg PL, Shanahan CM: Human vascular smooth muscle cells undergo vesicle-mediated calcification in response to changes in extracellular calcium and phosphate concentrations: A potential mechanism for accelerated vascular calcification in ESRD. *J Am Soc Nephrol* 15: 2857–2867, 2004
27. Libby P: Inflammation in atherosclerosis. *Nature* 420: 868–874, 2002

28. London GM, Guerin AP, Marchais SJ, Metivier F, Pannier B, Adda H: Arterial media calcification in end-stage renal disease: Impact on all-cause and cardiovascular mortality. *Nephrol Dial Transplant* 18: 1731–1740, 2003
29. Moe SM, O'Neill KD, Duan D, Ahmed S, Chen NX, Leapman SB, Fineberg N, Kopecky K: Medial artery calcification in ESRD patients is associated with deposition of bone matrix proteins. *Kidney Int* 61: 638–647, 2002
30. Schurgers LJ, Spronk HM, Soute BA, Schiffers PM, DeMey JG, Vermeer C: Regression of warfarin-induced medial elastocalcinosis by high intake of vitamin K in rats. *Blood* 109: 2823–2831, 2007
31. Johnson RC, Leopold JA, Loscalzo J: Vascular calcification: Pathobiological mechanisms and clinical implications. *Circ Res* 99: 1044–1059, 2006
32. Jersmann HP, Dransfield I, Hart SP: Fetuin/alpha2-HS glycoprotein enhances phagocytosis of apoptotic cells and macropinocytosis by human macrophages. *Clin Sci (Lond)* 105: 273–278, 2003
33. Tintut Y, Alfonso Z, Saini T, Radcliff K, Watson K, Bostrom K, Demer LL: Multilineage potential of cells from the artery wall. *Circulation* 108: 2505–2510, 2003
34. Tintut Y, Patel J, Territo M, Saini T, Parhami F, Demer LL: Monocyte/macrophage regulation of vascular calcification in vitro. *Circulation* 105: 650–655, 2002
35. Eghbali-Fatourechi GZ, Lamsam J, Fraser D, Nagel D, Riggs BL, Khosla S: Circulating osteoblast-lineage cells in humans. *N Engl J Med* 352: 1959–1966, 2005
36. Mohler ER 3rd, Gannon F, Reynolds C, Zimmerman R, Keane MG, Kaplan FS: Bone formation and inflammation in cardiac valves. *Circulation* 103: 1522–1528, 2001
37. Aikawa E, Nahrendorf M, Figueiredo JL, Swirski FK, Shtatland T, Kohler RH, Jaffer FA, Aikawa M, Weissleder R: Osteogenesis associates with inflammation in early-stage atherosclerosis evaluated by molecular imaging *in vivo*. *Circulation* 116: 2841–5280, 2007
38. Morony S, Tintut Y, Zhang Z, Cattley RC, Van G, Dwyer D, Stolina M, Kostenuik PJ, Demer LL: Osteoprotegerin inhibits vascular calcification without affecting atherosclerosis in ldlr(−/−) mice. *Circulation* 117: 411–420, 2008
39. Piedrahita JA, Zhang SH, Hagaman JR, Oliver PM, Maeda N: Generation of mice carrying a mutant apolipoprotein E gene inactivated by gene targeting in embryonic stem cells. *Proc Natl Acad Sci U S A* 89: 4471–4475, 1992
40. Phan O, Ivanovski O, Nguyen-Khoa T, Mothu N, Angulo J, Westenfeld R, Ketteler M, Meert N, Maizel J, Nikolov IG, Vanholder R, Lacour B, Drueke TB, Massy ZA: Sevelamer prevents uremia-enhanced atherosclerosis progression in apolipoprotein E-deficient mice. *Circulation* 112: 2875–2882, 2005

See related editorial, "Vascular Calcification: The Three-Hit Model," on pages 1162–1164.